Electronic Theses and Dissertations

Spring 5-13-2022

A Microfluidic Assay for Single Cell Bacterial Adhesion Studies Under Shear Stress

Amanda Trusiak
Duquesne University

Follow this and additional works at: https://dsc.duq.edu/etd

Part of the Biomedical Devices and Instrumentation Commons, and the Molecular, Cellular, and Tissue Engineering Commons

A MICROFLUIDIC ASSAY FOR SINGLE CELL BACTERIAL ADHESION STUDIES

UNDER SHEAR STRESS

A Thesis

Submitted to the John G. Rangos School of Health Science

Duquesne University

In partial fulfillment of the requirements for

the degree of Master of Science

By

Amanda Trusiak

May 2022

A MICROFLUIDIC ASSAY FOR SINGLE CELL BACTERIAL ADHESION STUDIES

UNDER SHEAR STRESS

By

Amanda Trusiak

Approved March 28, 2022

_____
Dr. Melikhan Tanyeri
Assistant Professor
Department of Engineering
(Committee Chair)

_____
Dr. Kimberly Williams
Associate Professor
Department of Engineering
(Committee Member/Reader)

_____
Dr. Gerard Magill
Vernon F. Gallagher Chair & Professor in
Healthcare Ethics
Center for Global Health Ethics
(Committee Member/Reader)

_____
Dr. Bin Yang
Assistant Professor
Department of Engineering
(Committee Member/Reader)

_____
Dr. Fevzi Akinci
Dean, Rangos School of Health Sciences
Professor of Health Administration and
Public Health

_____
Dr. John A. Viator
Chair, Department of Engineering
Professor of Engineering

ABSTRACT

A MICROFLUIDIC ASSAY FOR SINGLE CELL BACTERIAL ADHESION STUDIES

UNDER SHEAR STRESS

By

Amanda Trusiak

May 2022

Thesis supervised by Dr. Melikhan Tanyeri

The study of bacterial adhesion to host cells is important in understanding bacterial pathogenesis and developing new therapeutic approaches. Here, we studied bacterial adhesion under shear stress using a novel microfluidic method. Specifically, the adhesion of a uropathogenic *E. coli* strain (FimHOn, ATCC 700928/CFT073) to mannose-modified substrates was studied under flow conditions. The FimHOn *E. coli* strain expresses FimH which is a mannose-specific adhesin found on the fimbriae that binds to glycoproteins on the epithelium. We developed a microfluidic method that mimics bacterial adhesion to urothelial cells. First, the microfluidic channels were modified by sequentially adsorbing BSA-mannose and BSA onto channel surfaces. Bacterial solutions were then introduced to the microfluidic channels and bacterial interactions with the modified surface were imaged at 5 fps for 2 minutes using phase contrast microscopy under flow conditions. Manual tracking and TrackMate extensions of

ImageJ were used to analyze and quantify surface adhesion of bacteria on the simulated epithelial surface. Bacteria-surface interactions were studied with substrates modified using 8.3µg/mL, 16.7µg/mL, and 25.0µg/mL BSA-mannose solutions. Through image analysis, the percentage of bacteria interacting with the surface and the total interaction times were determined. The results indicated that as mannose concentration increased the average transient adhesion time and percentage of bacteria adhered to the surface also increased. It was also observed that bacteria permanently attached to the surface increased with time. Overall, our results show that FimHOn *E. coli* specifically and transiently interacts with the mannose-modified surface. By mimicking molecular interactions and flow-induced shear stress within the gastrointestinal, respiratory, and urogenital tracts, our microfluidic platform may help explain mechanisms underlying bacterial infections at the mucosal epithelium. Overall, our microfluidic approach provides a favorable platform to study bacterial host cell interactions to enable drug discovery and testing.

ACKNOWLEDGEMENT

TABLE OF CONTENTS

Chapter 3: Results

Chapter 4: Discussion and Future Work

LIST OF FIGURES

LIST OF ABREVIATIONS

E. coli – Escherichia coli

UTI – Urinary Tract Infection

UPEC – Uropathogenic Escherichia coli

IBD – Inflammatory Bowel Disease

AIEC – Adherent-Invasive Escherichia coli

AFM – Atomic Force Microscopy

PGMEA – Propylene Glycol Methyl Ether Acetate

PDMS – Polydimethylsiloxane

UV – Ultraviolet

NB – Nutrient Broth

DI – Deionized

BSA – Bovine Serum Albumin

PBS – Phosphate-Buffered Saline

ANOVA – Analysis of Variance

CHAPTER 1

INTRODUCTION

1.1 Bacterial Adhesion

Bacterial adhesion to the mucosal surface within the gastrointestinal, respiratory, and urogenital tracts allow bacteria to colonize host epithelium (Martino, 2018). Adhesion is critical in bacterial pathogenesis, occurring prior to invasion and the secretion of toxins (Letourneau et al., 2011). Bacteria express adhesins that promote binding to receptor proteins or polysaccharides present on epithelial cell surfaces. Adhesins are virulence factors that allow pathogenic bacteria to specifically adhere to host cells. These adhesins are found on bacterial fimbriae, which are subunit structures that extend from the bacterial cell surface (Schmidt et al., 2004). Fimbriae allow for adhesion to host cells and are directly responsible for the virulence of some bacterial pathogens (Mol et al., 1996). The FimHOn *E. coli* strain expresses FimH which is a mannose-specific adhesin found at the tip of the fimbriae. FimH is specifically found on type I bacterial pili (Tuson et al., 2013). This allows the *E. coli* to specifically bind to mannosylated glycoproteins on the surface of epithelial cells (Kline et al., 2009). FimH specifically binds to glycoprotein receptors that contain monomannose and trimannose. This interaction with cellular receptors initiates bacterial adhesion (Pizarro-Cerdá et al., 2006).
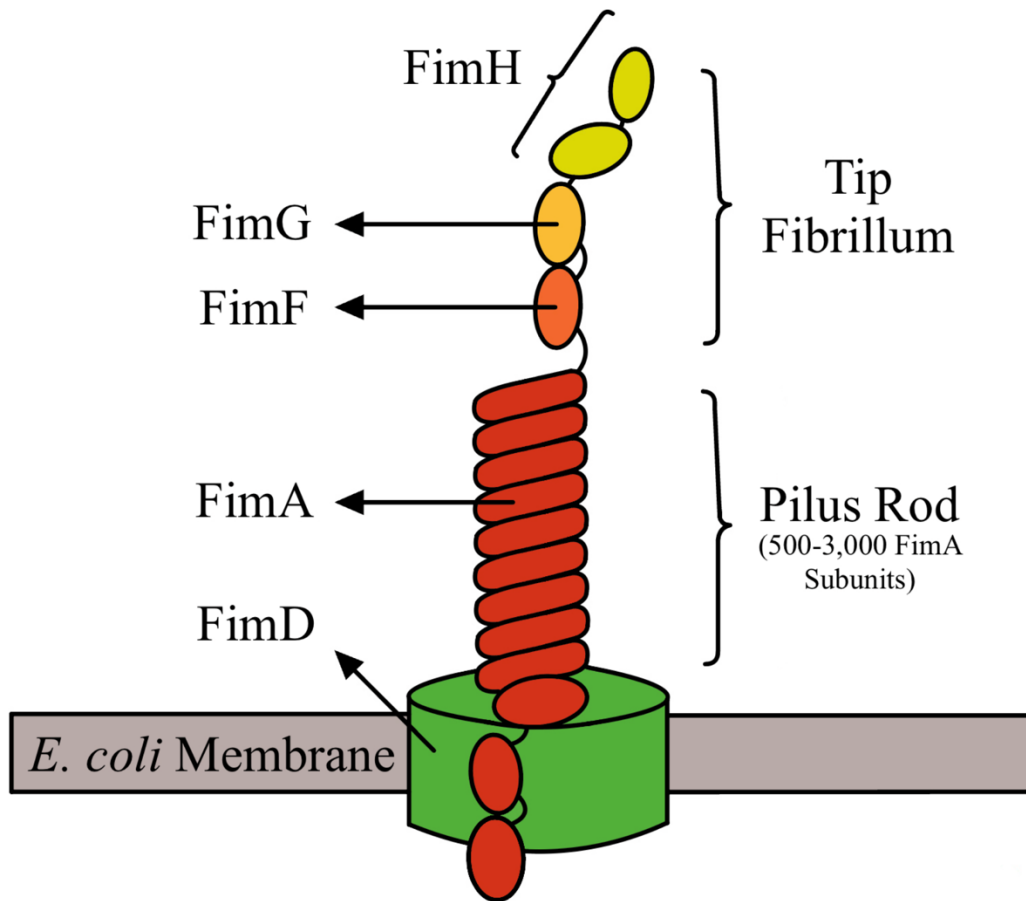
Figure 1 *Subunits of FimHOn E. coli Fimbriae:* Visualization of the FimH adhesin being expressed at the tip of the *E. coli* fimbriae.

The FimH adhesin has a pilin domain that anchors to the fimbriae and a lectin domain that recognizes mannose residues on mammalian cells (Tchesnokova et al., 2011). Interactions between bacteria and host cells are reinforced by shear stress. Catch-bonds play an important role by permitting the capture and retention of bacteria on the epithelium under flow conditions (Sauer et al., 2016). These catch bonds are strengthened by tensile mechanical forces (Yakovenko et al., 2008). *E. coli* displays stick-and-roll adhesion where the bacterium switches between rolling adhesion and stationary adhesion (Figure 2). The length of time bacteria demonstrates stationary adhesion can drastically differ from milliseconds to hundreds of seconds.

This stick-and-roll adhesion allows for rapid colonization under ideal stress conditions (Thomas, 2008). Understanding bacterial adhesion at the single cell level will aid in overall understanding of bacterial infections and help develop new therapeutic approaches.
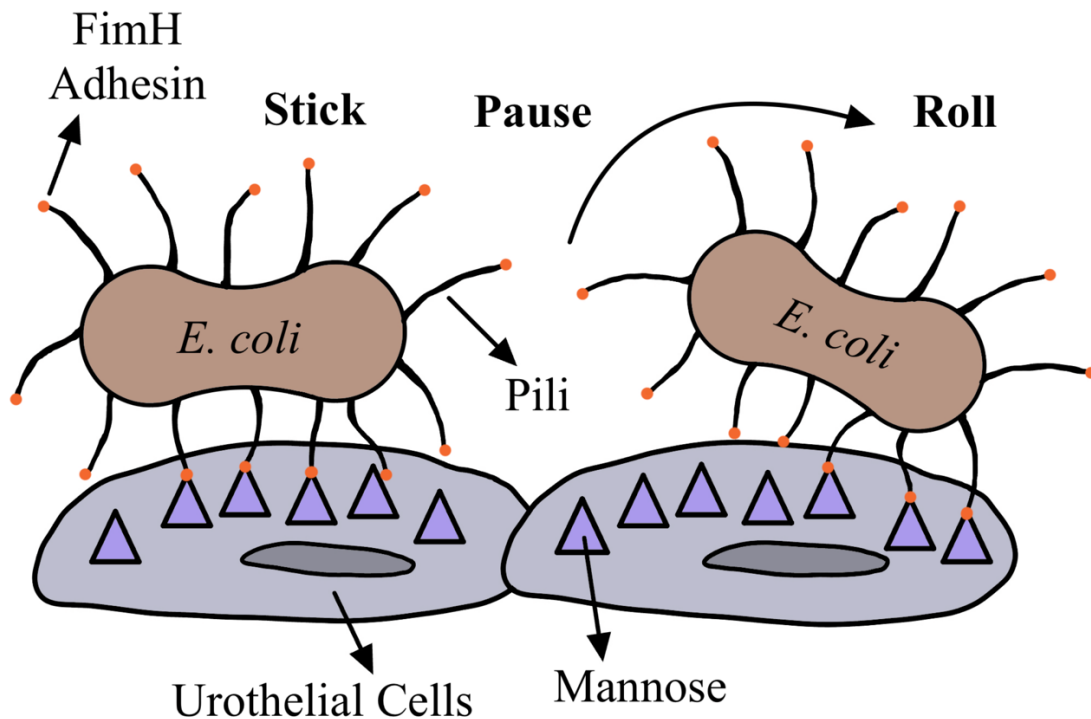
Figure 2 *Stick and Roll Adhesion:* A visual representation of *E. coli* interacting with urothelial cells utilizing stick and roll adhesion.

1.2 Urinary Tract Infection

Urinary tract infections are considered one of the most common bacterial infections, and pathogenic *E. coli* strains directly contribute to the prevalence of UTIs (Flores-Mireles et al., 2015). It is estimated that around 50-60% of women report having at least one UTI in their lifetime. Within the United States UTIs account for 7 million office visits, 1 million emergency department visits, and over 100,000 hospitalizations (Foxman, 2002). UTIs can affect the

kidneys, ureters, bladder, and urethra and have symptoms such as a burning sensation when urinating, lower abdomen discomfort, back or side pain, high fever, nausea, and vomiting (Chu et al., 2018). Individuals experiencing a UTI may have complications such as recurring infections, kidney damage, urethral narrowing, and sepsis. Uropathogenic *E. coli* (UPEC) strains are the most frequent pathogens responsible for UTI's. Most pathogenic strains of *E. coli* exhibit mannose-sensitive fimbriae which can attach to human urinary tract epithelial cells (Edén et al., 1981). Among UPEC adhesion, the FimH adhesin is a major determinant of virulence (Hojati et al., 2015). The main receptor of the FimH adhesin in the urinary tract is monomannose contained in glycoproteins on the cell surface. This FimH interaction with bladder epithelial cells triggers a signal transduction cascade resulting in the uptake of bacteria and chronic urinary tract infections (Pizarro-Cerdá et al., 2006). Once *E. coli* attaches to the mucosal surface it can colonize and infect the area. Understanding *E. coli* adhesion to human urinary tract epithelial cells is essential to understanding UTIs and developing innovative anti-adhesive and prophylactic approaches to prevent UTIs (Terlizzi et al., 2017).

1.3 Inflammatory Bowel Disease

A very diverse range of microbial species reside in the human intestinal tract. This microbiota enhances the intestinal epithelial barrier and aids in the development of the immune system (Kamada et al., 2013). Immune responses to environmental triggers can cause inflammation within the gastrointestinal tract. It is commonly hypothesized that chronic inflammation caused by dysbiosis in the intestinal microbiota can result in Inflammatory Bowel Disease (IBD) (Tamboli et al., 2004). IBD is a chronic condition that encompasses Crohn's disease and ulcerative colitis (de Souza et al., 2016). An individual who has developed IBD can

experience symptoms such as diarrhea, fatigue, abdominal pain, blood present in stool, and a reduced appetite. The disease could also cause complications such as bowel obstruction due to the thickening of the intestinal wall (Fakhoury et al., 2014). Adherent invasive *E. coli* (AIEC) has been increasingly implicated in the pathogenesis of IBD. AIEC strains predominantly express the FimH adhesin allowing them to bind to intestinal epithelial cells (Palmela et al., 2018). This FimH expression is considered to be critical in the development of IBD (Dreux et al., 2013). Many studies have shown that the intestinal mucosa of some IBD patients is abnormally colonized by *E. coli* strains with adherent and invasive properties (Costa et al., 2020). Creating an *in vitro* model of intestinal bacteria-epithelial interactions can further the general understanding of IBD and help develop mechanism-based treatment strategies.

1.4 Methods for Studying Bacterial Adhesion at the Single Cell Level

1.4.1 Atomic Force Microscopy

Two primary methods for investigating bacterial adhesion at the single cell level are Atomic Force Microscopy (AFM) and optical tweezers. AFM utilizes a cantilever with an adhesin-specific coated bead attached to the tip (Gavara, 2017). Bacteria are immobilized onto a rigid substrate such as silicon or glass. The cantilever tip is then brought into contact with the bacterium, and the attachment force is measured by pulling upward on the bacterium until the bond breaks (Figure 3). AFM measurements are performed without the cantilever tip touching the surface as to avoid contamination. Scanning electron microscopy is performed on the tip of the cantilever after the force measurement to ensure the presence of bacteria. A force curve is recorded as the bond between the bacteria and the substrate is broken (Razatos et al., 1998). This

enables the investigation of kinetics and strength of binding interactions between bacteria and epithelial cells (Gavara, 2017).
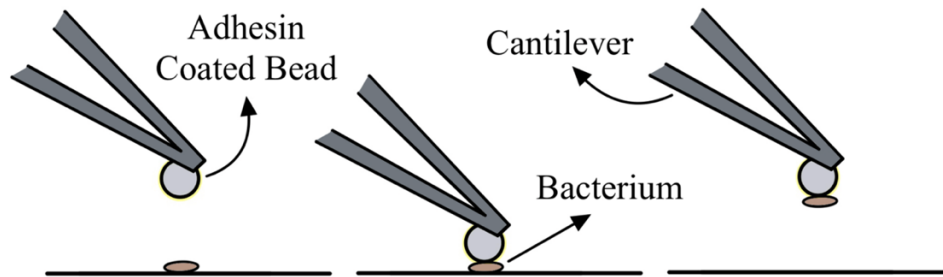
Figure 3 *Atomic Force Microscopy:* A schematic of AFM being utilized to measure the attachment force of a single bacterial cell to a target surface.

1.4.2 Optical Tweezers

Optical tweezers are also used to measure bacterial attachment force. With the use of an objective lens, infrared laser beams are tightly focused to capture and manipulate an adhesin specific coated bead. The bead is then brought into contact with bacteria. After contact is made, optical tweezers pull the bead away until the bacterial bond breaks, thereby measuring the attachment force (Figure 4). Optical tweezers also allow measurement of biophysical properties of bacterial adhesion.
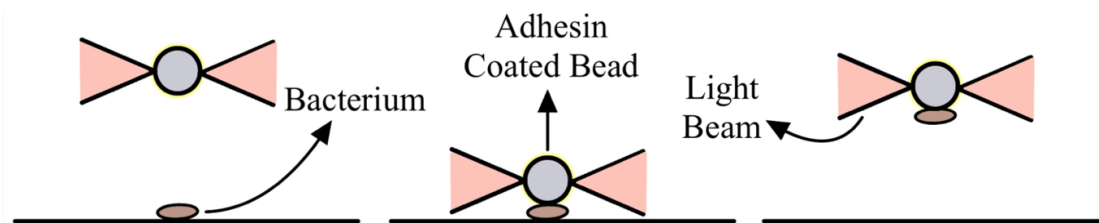
Figure 4 *Optical Tweezers*: A schematic of optical tweezers measuring the attachment force of a single bacterial cell.

1.4.3 Limitations of Current Methods

Both optical tweezers and AFM provide insights into how tight the molecular adhesion forces are between the microorganism and the host cells. However, bacterial transport and adhesion are heavily influenced by the presence of fluid flow in microbial habitats. Cell–cell adhesion often occurs under dynamic conditions and varying mechanical stress. As recently described, catch-bonds also play a major role in bacterial adhesion and infection, permitting the capture or retention of cells under flow conditions (Sauer et al., 2016). Within the intestinal tract, luminal flow impacts adhesion to the gut epithelium and the growth of pathogenic bacteria (Secchi et al., 2020). Therefore, it is essential to mimic the first step in the bacterial pathogenesis in pulmonary, gastrointestinal, and urinary infections, which is the adhesion to epithelial cells under flow conditions. While AFM and optical tweezers are useful in quantifying binding forces and kinetics, both methods lack the ability to investigate adhesion events under shear stress conditions. Studying bacterial adhesion under physiologically relevant conditions is essential in explaining molecular mechanisms underlying infections.

1.5 Microfluidic Devices

Microfluidic devices enable observation of bacterial interactions under aqueous flow conditions. For example, microfluidic devices have been used to study the effect of culture media content on biofilm formation under the presence of fluid flow (Straub et al., 2020). Microfluidic devices have also been used to observe the effect of shear rate on adhesion of fibroblast cells (Lu et al., 2004). To study bacterial adhesion on mucosal surfaces, we developed a novel microfluidic method. The microfluidic platform allows bacteria to be introduced at a constant velocity (or shear rate) into a microchannel and adhere to the walls of the channel, thereby

mimicking adhesion to urothelial cells. Using this platform, we studied transient interaction times as well as the impact of surface-immobilized mannose concentration on adhesion. Microfluidic devices allow for cost-effective, precisely controlled experiments that utilize very small sample sizes. Microfluidic devices feature sizes that are comparable to microorganisms, thereby providing an additional advantage to study bacterial adhesion at the single cell level. Furthermore, microfluidic devices are disposable, which minimizes the risk of contamination for these studies (Streets et al., 2013). A microfluidic device with straight channels was chosen for its simplicity (Figure 5). Each microfluidic channel was 20mm long, 200µm wide and 50µm in height. The device was composed of a PDMS slab on the top, and a glass substrate on the bottom. The bottom glass surface of the channel allows for better imaging when observing bacterial interactions by brightfield and phase contrast microscopy.
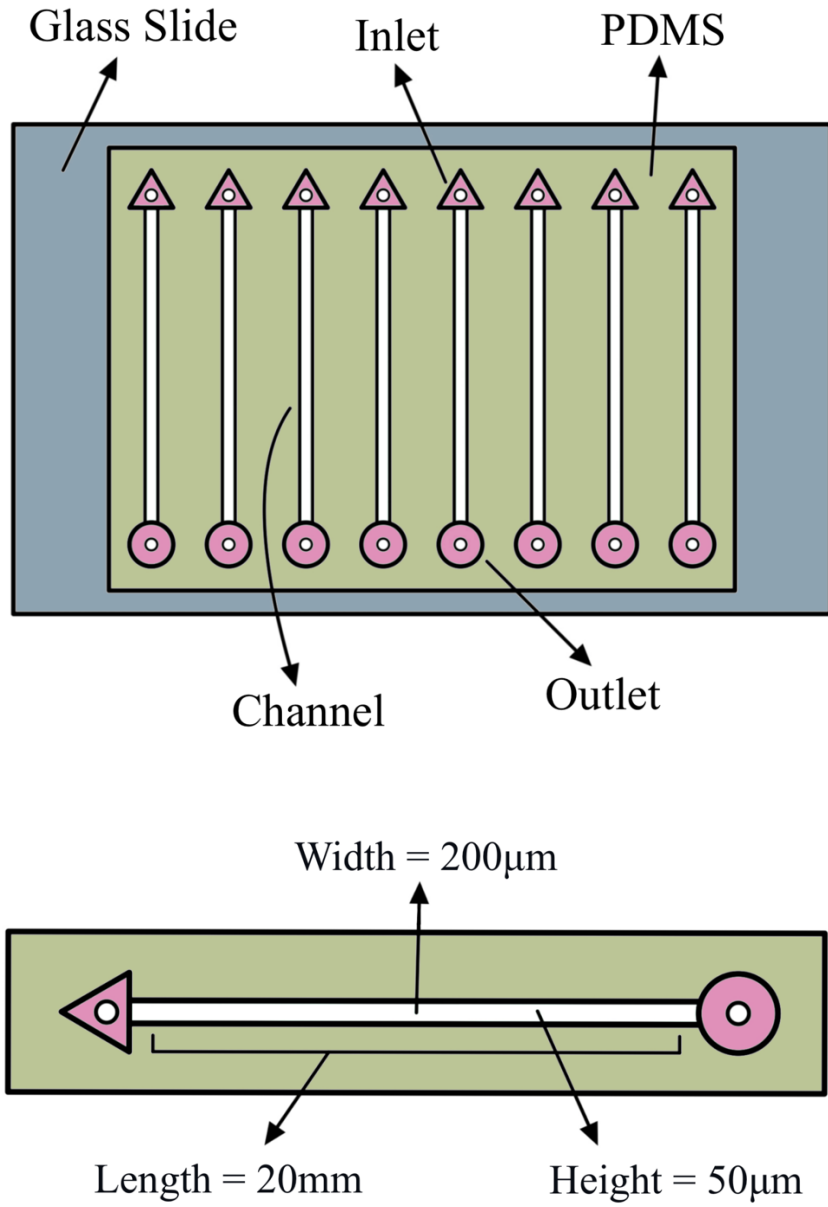
Figure 5 *Microfluidic Device Design:* The microfluidic design for bacterial adhesion studies. Each individual channel had a length of 20mm, a height of 50μm, and a width of 200μm.

CHAPTER 2

METHODS

2.1 Microfluidic Device Fabrication

Fabrication of microfluidic devices was carried out in a Class 1000 clean room using photolithography and soft lithography techniques. The fabrication process started with a silicon wafer to create the SU-8 mold. First, silicon wafers were cleaned with acetone and isopropyl alcohol and dried with compressed air. The wafer was spin-coated with SU-8 2050 with a feature height of ~50µm. The spin coating process involved three steps: a spread step at 500 rpm for 5-10 seconds with an acceleration of 100 rpm/second, a coating step at 2000 rpm for 30 seconds with a ramp of 300 rpm/second, and a slowdown step at 500 rpm/second. The wafer was then soft baked at 65°C for 3 minutes and at 95°C for 9 minutes.

The next step was photolithography where a mask containing the device features was placed over the wafer. A quartz slab was placed on top of the mask to bring the mask in conformal contact with the SU-8. The wafer was then exposed to UV light for 11 seconds. A long pass filter was used to eliminate UV radiation below 350nm. After UV exposure, the wafer was baked at 65°C for 2 minutes and at 95°C for 7 minutes. Once the baking was complete, the image of the mask was visible in the photoresist. The wafer was immersed in a solvent-based developer, PGMEA, and was agitated and swirled for approximately 7 minutes to fully remove any uncross-linked SU-8. The wafer was then rinsed with isopropyl alcohol and dried with compressed air.

After the wafer was thoroughly cleaned, it was silanized to prepare for replica molding. A few drops of silane were added to a petri dish and placed within a vacuum desiccator with the

silicon wafer containing the SU-8 mold. The wafer was incubated with vaporized silane under vacuum for approximately 15 minutes. PDMS was then prepared by combining the base and the cross-linker components at a 10:1 ratio. The PDMS was placed into a vacuum desiccator to remove all the air bubbles from the mixture. The PDMS was then poured onto the wafer in the petri dish and any residual bubbles were carefully removed. The wafer with the uncross-linked PDMS layer was then placed into the oven at 75°C overnight. After the curing is complete, the PDMS slab was removed from the wafer using a scalpel. Holes were punched into the PDMS at the inlet and outlet of each channel using a 22-gauge needle. A glass slide was cleaned prior to bonding using acetone and isopropyl alcohol, and the PDMS slab containing the device features was cleaned using tape to remove any debris. The glass slide and PDMS with the device features facing upward were placed inside a plasma chamber, and plasma was generated at a power of 30W for approximately 20 seconds. After the oxygen plasma treatment, the PDMS slab and glass slide were brought into conformal contact to obtain an impervious seal between the two layers. The bonded device was placed back in the oven at 75°C before use in experiments.
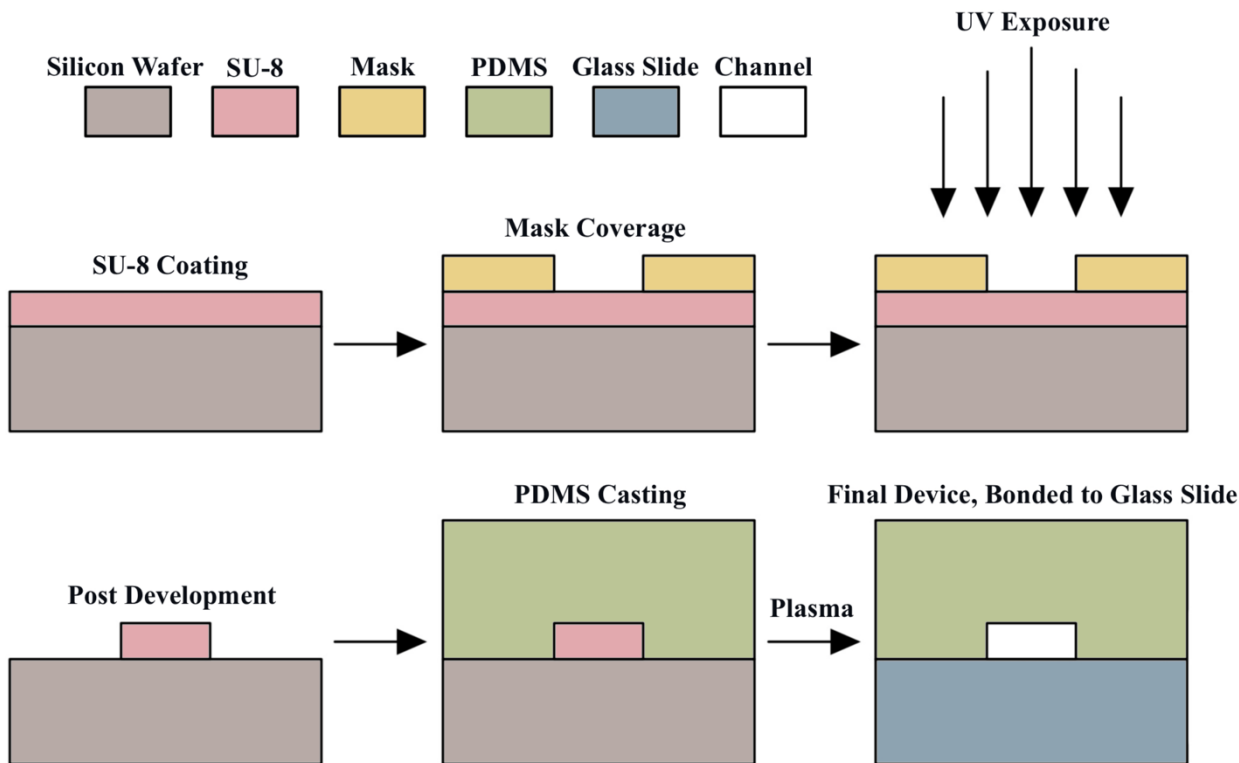
Figure 6 *Steps of Microfluidic Device Fabrication:* A visualization of the fabrication process of microfluidic devices utilizing photolithography and soft lithography techniques.

2.2 Bacteria Culture

The FimHOn ATCC 700928/CFT073 *E. coli* strain was chosen because it has been engineered to constantly express the FimH adhesin. The expression of FimH enabled investigation of bacteria-surface interactions for prolonged time scales. Culturing this strain of bacteria occurred over a 2-day static incubation period. Nutrient broth (Beef extract, 3.0 g/L Peptone, 5.00 g/L) was prepared using 8g of NB powder and 1L of DI water. The container was agitated until the powder was completely dissolved and the mixture was sterilized through autoclaving for 15 minutes at 121°C.

The FimHOn ATCC 700928/CFT073 *E. coli* strain was cultured from glycerol stocks

stored at -80°C. Cultures were started by transferring 3μL of bacterial glycerol stock into a test

tube with 8mL of nutrient broth using standard aseptic techniques. A separate test tube

containing uninoculated media was used as a control for contamination. The cultures were

statically incubated at 37°C for 24 hours. The next day, the medium was refreshed by

transferring 800μL of cultured bacteria into a culture tube containing 7.2mL of nutrient broth.

The samples were statically incubated at 37°C for another 24 hours. After this incubation period,

bacterial cultures were diluted and used in experiments.

The bacterial concentration was determined by measuring the optical densities of the

cultures using the Eppendorf BioPhotometer. Typical optical densities for bacterial cultures

ranged between OD_{600} = 1.0-1.2. The cultures were diluted before loading into syringes for

microfluidic bacterial adhesion experiments. The dilution factor was determined based on the

initial bacterial concentration in the culture (based on OD measurements) and average number of

bacteria per field of view. A typical dilution factor of 20x was used for a bacterial culture with

OD_{600} = 1.0. We adjusted the dilution factor to ensure a sufficient number of bacterial adhesion

events during data acquisition, while avoiding overcrowding of the field of view.

2.3 Microfluidic Assays

Bacterial adhesion experiments were performed by creating a simplified microfluidic

mimic of the gut epithelium. Specifically, microchannels are functionalized with bovine serum

albumin-mannose (BSA-mannose, Carbosynth) which serves as a binding site for the bacterial

adhesin FimH. The microchannels are further treated with bovine serum albumin (BSA) to block

nonspecific interactions between the bacteria and the walls of the microchannel. The BSA

solutions were prepared with 90μL of phosphate-buffered saline (PBS) and 5μL of 5mg/mL

BSA. BSA-mannose solutions at various concentrations (8.3μg/mL, 16.7μg/mL, and 25.0μg/mL

of BSA-mannose in PBS) were used to promote FimH specific binding to the channel surface.

The 8.3μg/mL BSA-mannose solution was prepared with 90μL of PBS, 5μL of 5mg/mL BSA

solution, and 5μL of 2.5μM BSA-mannose solution. Similarly, 16.7μg/mL and 25.0μg/mL BSA-

mannose solutions were prepared by adding 10μL and 15μL of 2.5μM BSA-mannose solution

into 5μL of 5 mg/mL BSA solution and 85μL and 80μL of PBS, respectively. FimHOn *E. coli*

was prepared at a 20x dilution with nutrient broth by diluting 50μL of cultured bacteria into

950μL of nutrient broth for experiments.

2.4 Agglutination Assay

Agglutination tests were performed to confirm expression of FimH. The expression of

bacterial adhesins is often validated by the ability of the bacteria to agglutinate yeast cells

(Figure 7, left panel). Both adherence and agglutination entail expression of bacterial pili (Eshdat

et al., 1981). Here, we performed a yeast agglutination assay to demonstrate expression of

bacterial adhesins by the *E. coli* strain used in the experiments. Yeast is used because the cell

surface glycans contain mannose, a target for the FimH adhesin. First, a 0.1% yeast stock

solution was prepared by adding 0.01g of yeast into 10mL of PBS. The mixture was gently

shaken until the yeast dissolved. The yeast solution was incubated in a water bath at 37°C for 20

minutes to activate and release yeast cells. After blooming, the tube was gently agitated again to

ensure all live yeast cells had been uniformly dispersed into the solution.

A 1% crystal violet stock solution was prepared by dissolving 0.1g of crystal violet into

10mL of PBS to stain bacteria and yeast cells. Furthermore, 1mL of cultured bacteria was

centrifuged for 5 minutes at 5000rpm. The supernatant was gently removed, and the bacterial pellet was resuspended in 200μL of PBS. This washing steps was repeated 3 times to ensure complete removal of bacterial growth medium. Furthermore, 2.5mL of yeast stock solution and 50μL of the crystal violet stock solution were pipetted into 15mL falcon tubes.

For the agglutination assay, bacterial solution in PBS was serially diluted (2x) along the rows of a 96 well plate such that each well contains 50μL of the sample. Next, 150μL of crystal violet stained yeast solution was added to each well. After a 5-minute incubation period, the agglutination of yeast by mannose-specific bacterial lectins (FimH) was examined under the microscope at 4x magnification. We observed that the statically cultured FimHOn ATCC 700928/CFT073 *E. coli* strain resulted in yeast agglutination, suggesting expression of the FimH adhesin. As a control experiment, we conducted agglutination experiments where we added a mannose substitute, methyl α-D-mannopyranoside, to each well. In the presence of excess methyl α-D-mannopyranoside, bacterial adhesins were occupied, thereby hindering their ability to agglutinate yeast cells (Figure 7, right panel). We observed that yeast agglutination of FimHOn *E. coli* was inhibited by the addition of excess methyl α-D-mannopyranoside, further confirming that agglutination was due to mannose-specific FimH binding.
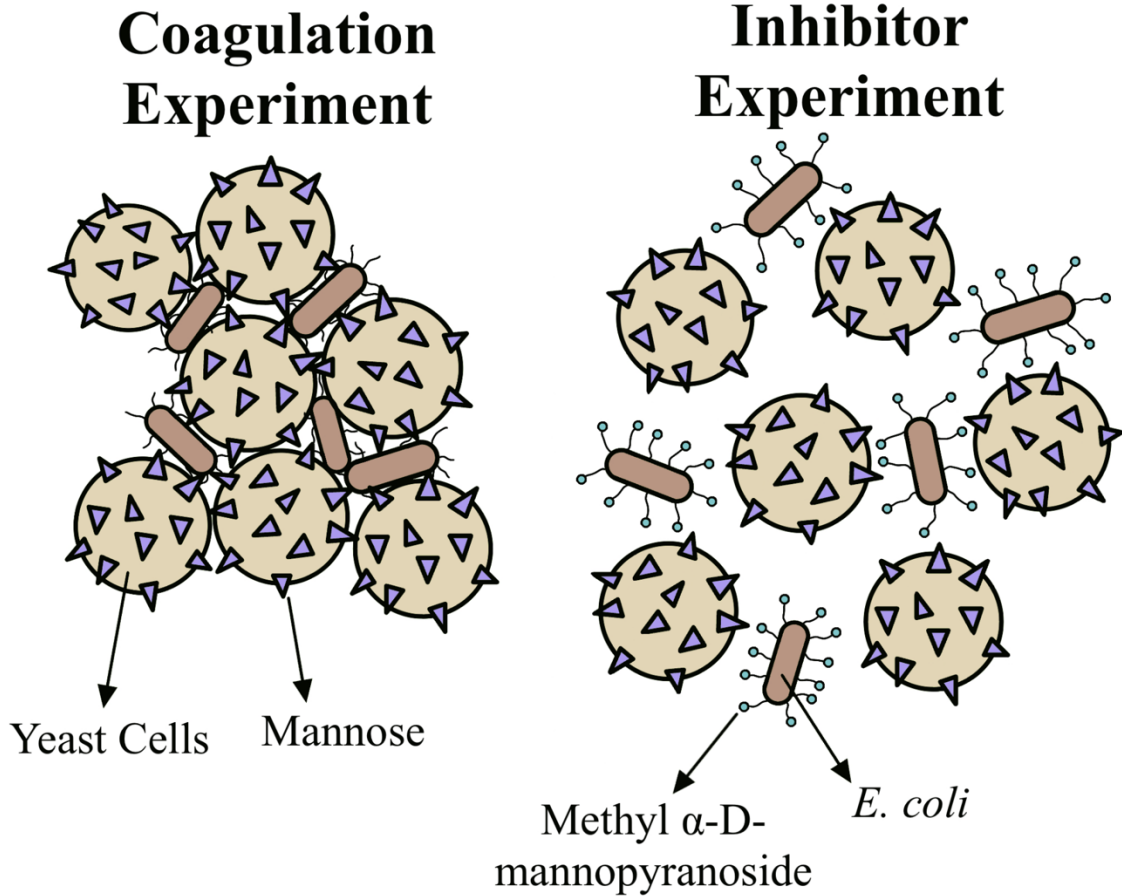
Figure 7 *Agglutination Assay:* Yeast cells are clumped together by *E. coli* adhesion in the coagulation experiment (left), while Methyl α-D-mannopyranoside prevents adhesion and clumping (right).

2.5 Experimental Procedure

The experimental setup consisted of a microfluidic device, a syringe pump (Harvard Apparatus Pump 11 Elite, 70-4505), an inverted research microscope (Nikon Ti2-E) equipped with 20x and 40x phase contrast objective lenses, and a CCD camera (Basler acA1920-155um) (Figure 8 and 9).
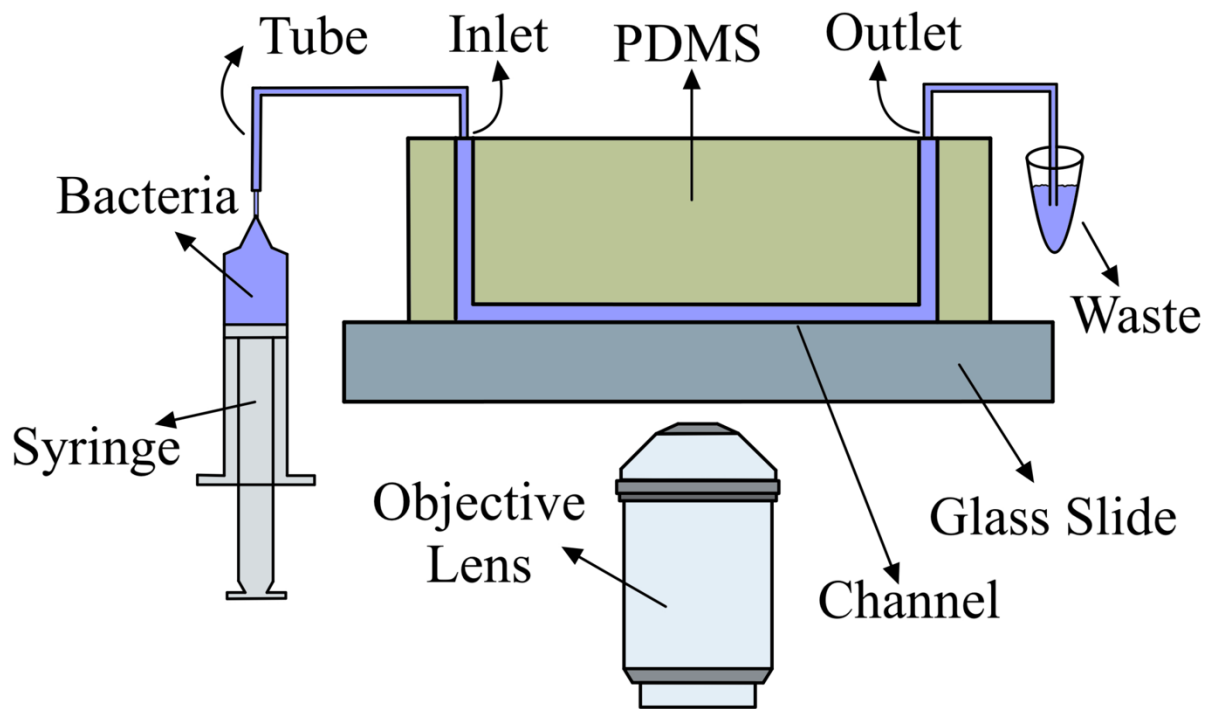
Figure 8 *Schematic of the Experimental Setup:* Experiments consisted of bacteria flowing through the microfluidic device at a constant velocity while monitoring adhesion to the simulated gut epithelial surface. Phase contrast microscopy was used to capture images of bacteria interacting with the microfluidic surface.
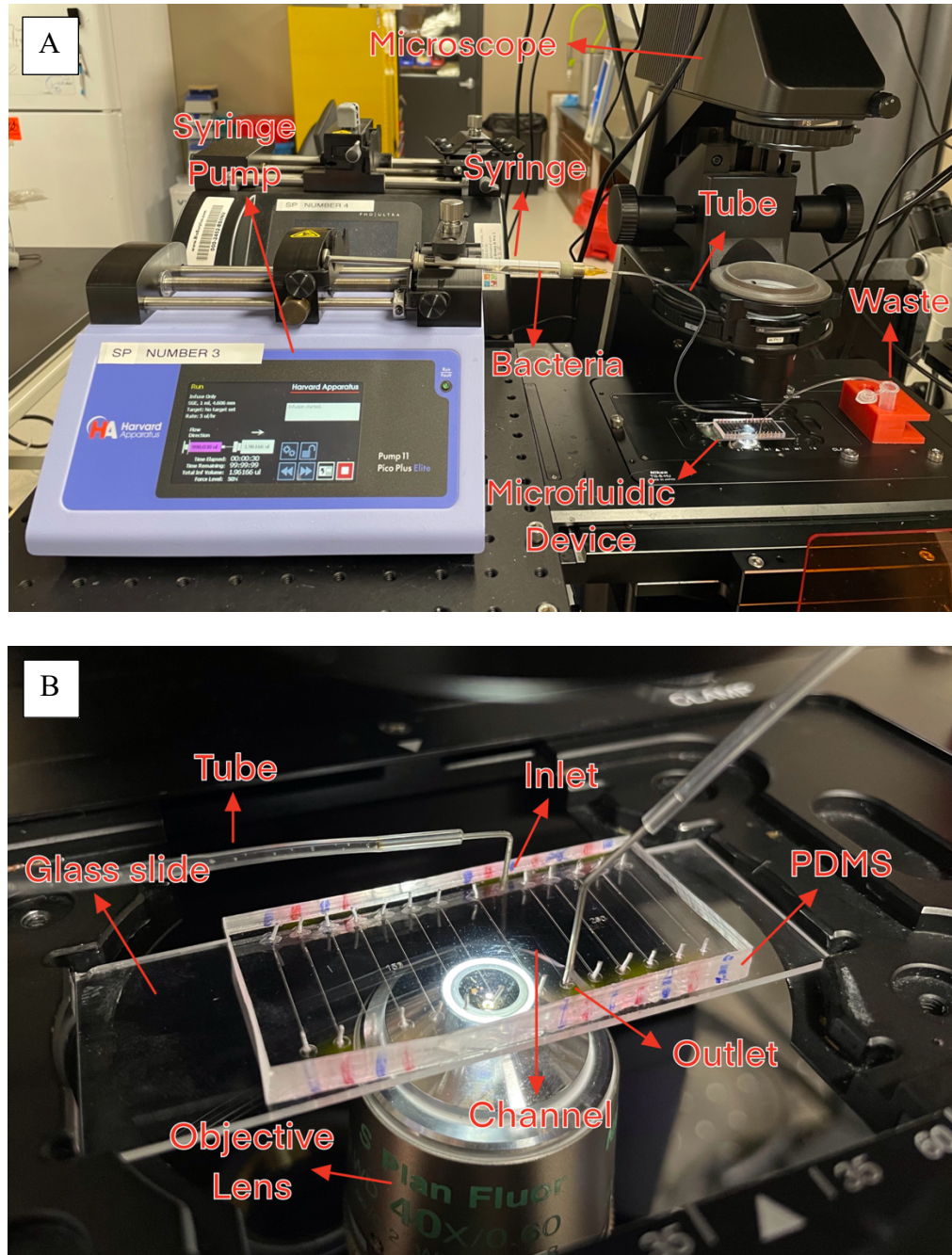
Figure 9 *Image of the Experimental Setup:* (A) The syringe pump was used to introduce bacteria into the microfluidic device at a constant flow rate. Bacterial interactions were then captured using the microscope equipped with a CCD camera. (B) A closeup view of the microfluidic device mounted on the microscope stage. Tubing was connected to the inlet and outlet of the device channel allowing bacteria to flow through.

Bacterial solutions were introduced into a microchannel functionalized with BSA-mannose, and the interaction of the bacteria with the surface was imaged using phase contrast microscopy. For the bacterial adhesion experiments, the microchannels within the microfluidic device were modified with BSA and BSA-mannose (Figure 10). First, 10μL of PBS was flown into the microchannel. The channel was then flushed with either 10μL of the BSA solution or 10μL of one of the BSA-mannose solutions. The device was then incubated at room temperature for 10 minutes to enable adsorption of proteins to microchannel surfaces. After the incubation period was complete, the channel was flushed with 10μL of PBS to remove excess protein from the microchannel. While the BSA-mannose assays promoted bacterial adhesion to the surface, a BSA-only assay was carried out as a control experiment.
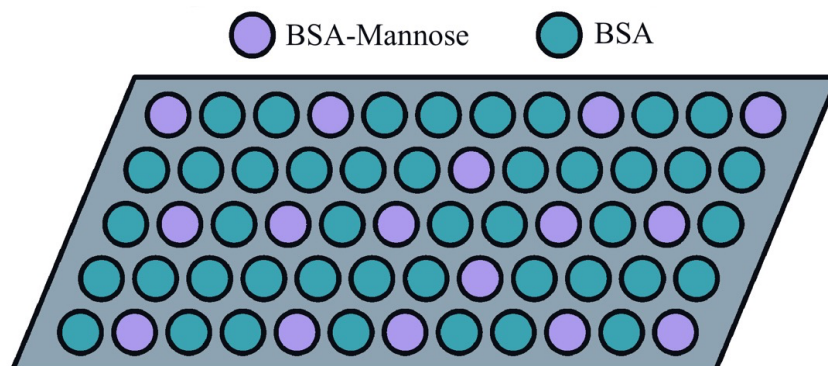
Figure 10 *Adsorption of BSA and BSA-Mannose to Microfluidic Device Surfaces:* A visualization of BSA and BSA-mannose being adsorbed onto the microfluidic device surface.

A 1 mL syringe (SGE 1MDF-LL-GT) was loaded with a 20x bacteria dilution, and all air bubbles were removed. To sterilize the syringe and prevent contamination prior to loading, the syringe was initially flushed with 1000μL of ethanol with the tubing attached. The syringe and

tubing were then flushed with 1000μL of PBS three times to thoroughly rinse out any trace of

ethanol. The syringe was mounted on the syringe pump and set up to run at 100μL/hr to prime

the microfluidic channel and eliminate any air bubbles to ensure consistent flow. The syringe

pump was then slowed down to 20μL/hr, and the outlet tubing was inserted into an Eppendorf

tube to collect the waste . Next, the flow rate was further reduced to 5μL/hr. Bacterial adhesion

events were imaged at the bottom surface of the microchannel at 60x magnification (40x lens

with additional 1.5x magnification) using phase contrast microscopy (Figure 11).
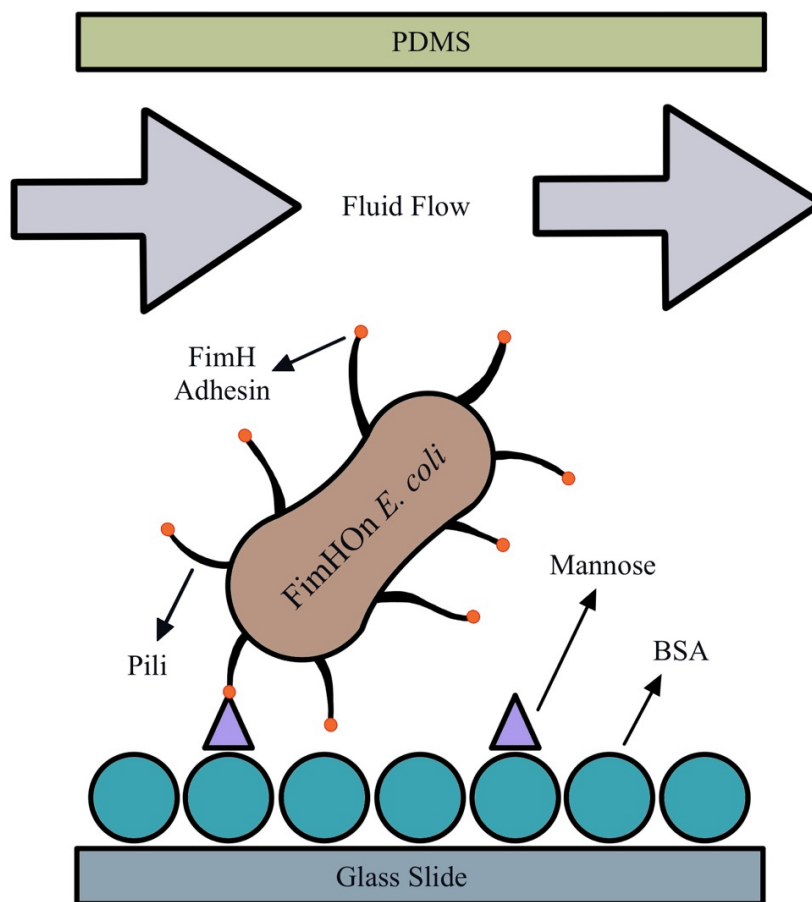
Figure 11 *Mannose-Specific Adhesion Between E. coli and the BSA-Mannose Modified Surface:*
A schematic of the FimH adhesin located on the pili of the *E. coli* specifically binding to BSA-
mannose immobilized on the microfluidic device surface.

Bacterial interactions with the surface, including transient and permanent binding events, were captured in real-time using a CCD camera (Basler acA1920-155um) mounted on the microscope. As the bacteria flowed through the channel and interacted with the surface-immobilized mannose, we captured 600 images (1920x1200 pixels) at 5 frames per second for a total of 2 minutes. Several image sets were obtained to ensure observation of numerous surface binding events.

2.6 Image Processing

Images captured in experiments were processed using ImageJ. First, images were converted into a stack. The magnification factor and pixel size (5.86 µm) were used to calculate the correct length scale on the images. Plugins such as TrackMate and Manual Tracking were then used to track bacterial trajectories along the microchannel and quantify bacterial interactions (Figure 12). TrackMate was used to track all bacteria within the field of view (and in focus) simultaneously (Tinevez et al., 2017). The images were binarized by determining an intensity threshold. Careful selection of the threshold enables tracking of most bacteria within the field of view. Erroneous trajectories were manually removed from the data. Upon quality control, bacterial interactions were quantified by determining the number of bacteria interacting with the surface as well as the duration of the interaction.

The Manual Tracking plugin was used to improve data accuracy on transiently interacting bacterium. Images were analyzed to identify and locate bacteria that briefly adhered to the surface. Detected trajectories were further examined manually frame by frame to ensure accuracy in interaction times and measurement of positions and displacement.
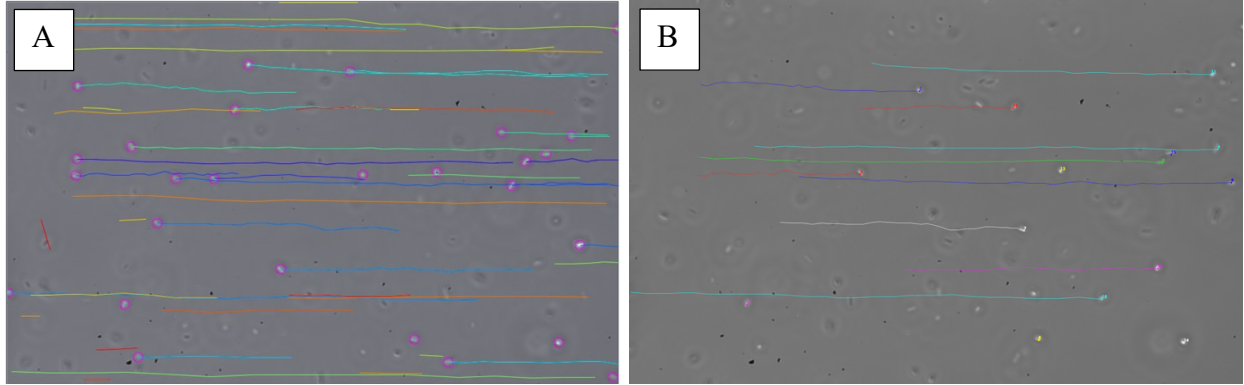
Figure 12 *Tracking Bacterial Interactions Using Image Processing Tools:* (A) Bacterial

interactions were analyzed using the TrackMate plugin of ImageJ tracking all bacteria within the

field of view (highlighted) simultaneously. (B) The trajectory of each transiently interacting

bacterium was inspected manually to ensure accuracy.

CHAPTER 3

RESULTS

3.1 Optical Density Results

Optical densities of the nutrient broth control and cultured bacteria solution were observed to quantify bacteria in each culture and determine a dilution factor for the bacterial adhesion experiments. The average optical density of the nutrient broth control was 0.0008 ± 0.0015, and the average optical density of the cultured bacteria was 1.10 ± 0.04. The average optical density readings were consistent throughout all experiments.

3.2 Agglutination Results
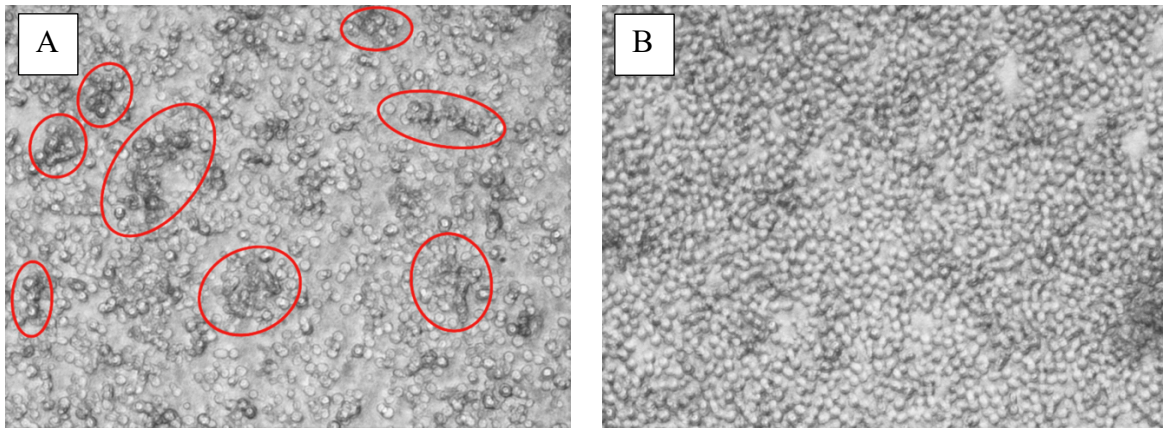
Figure 13 *FimHOn Yeast Agglutination Results:* (A) The control experiment in the presence of bacteria but not the FimH inhibitor shows the yeast cells noticeably clumping together. (B) The experiment with the FimH inhibitor, Methyl α-D-mannopyranoside, shows the yeast cells uniformly distributed, and not forming clumps.

To test the expression of FimH we conducted yeast agglutination assays with FimHOn *E. coli.* We anticipated that bacteria expressing FimH will exhibit mannose-sensitive yeast cell agglutination (Mirelman et al., 1980). We observed that the assay with FimHOn *E. coli* resulted in clumping of the yeast (*Saccharomyces cerevisiae*) cells by bacteria (Figure 13A). Furthermore, the assay with FimHOn *E. coli* in the presence of methyl α-D-mannopyranoside resulted in suppression of agglutination of yeast cells (Figure 13B). A control experiment with wild-type *E. coli* was also conducted and yielded minimal agglutination, further suggesting that the FimHOn *E. coli* was specifically binding to yeast cells (Firon et al., 1984). As a result, we conclude that the FimHOn *E. coli* strain expresses FimH and yields a mannose-specific agglutination of yeast cells.

3.3 Bacterial Interaction Types

To investigate bacterial adhesion to surfaces mimicking urothelium and gut epithelium, we observed the interaction of FimHOn *E. coli* strains with mannose modified microfluidic channels. Due to the shear dependent stick-and-roll adhesion of type I fimbriated *E. coli* with the surface (Thomas et al., 2004), we specifically observed bacteria that flow along and interact with the bottom surface of the microfluidic channel. While some bacteria did not interact with the surface (Figure 14A), others interacted for short (Figure 14B) and long (Figure 14C) durations, or were permanently attached to the surface (Figure 14D).
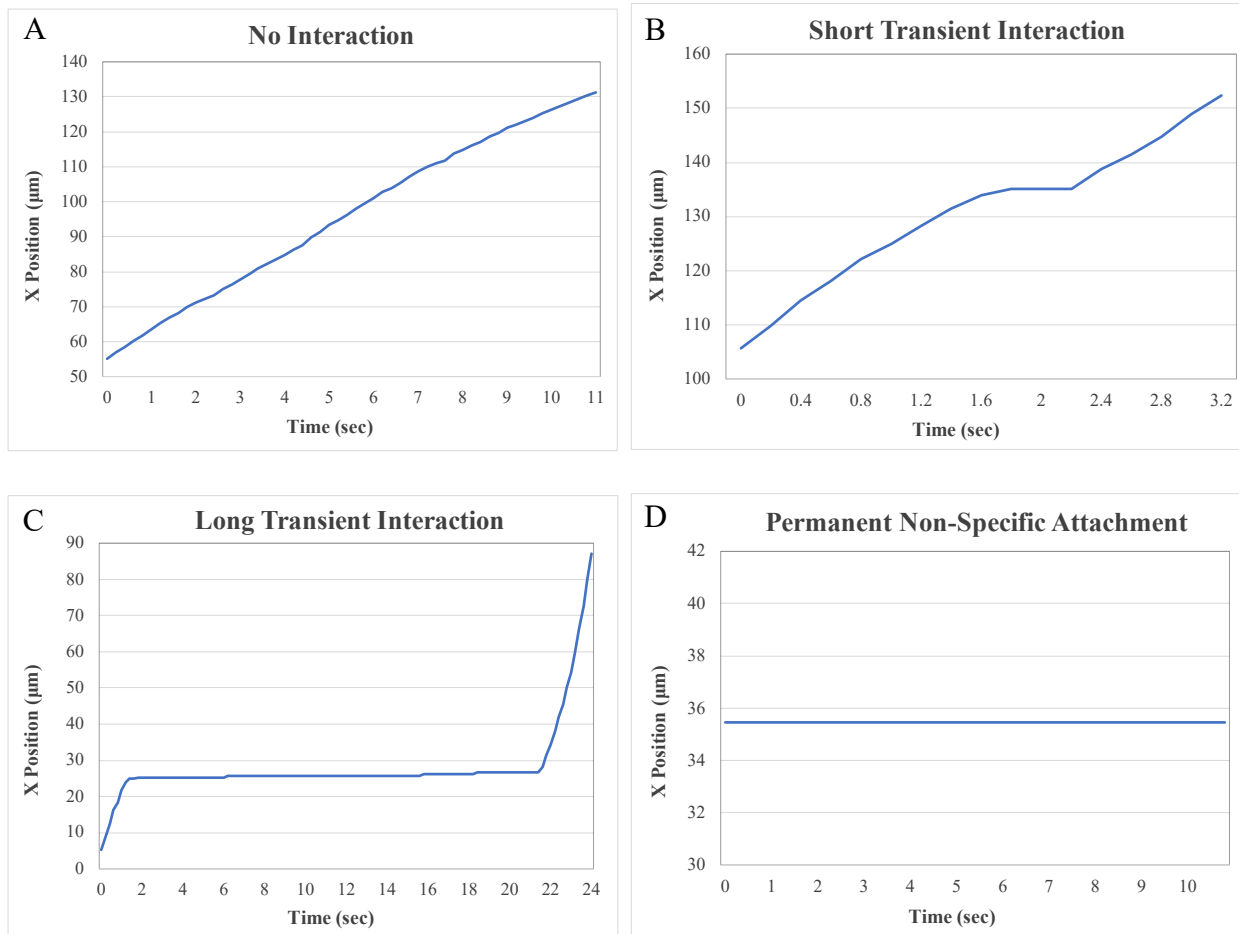
Figure 14 *Bacterial Interactions with Mannose Modified Microchannel Surface:* Sample bacterial traces for: (A) Non-interacting bacteria flowing at a constant velocity through the microchannel, (B) Bacteria exhibiting short transient interaction with the surface and continuing to flow through the device, (C) Bacteria exhibiting long transient interaction before detaching and continuing to flow through the device, and (D) Bacteria permanently adhered to the channel surface. Each plot represents the position of the bacteria along the channel length (and along the direction of the flow) as a function of time.
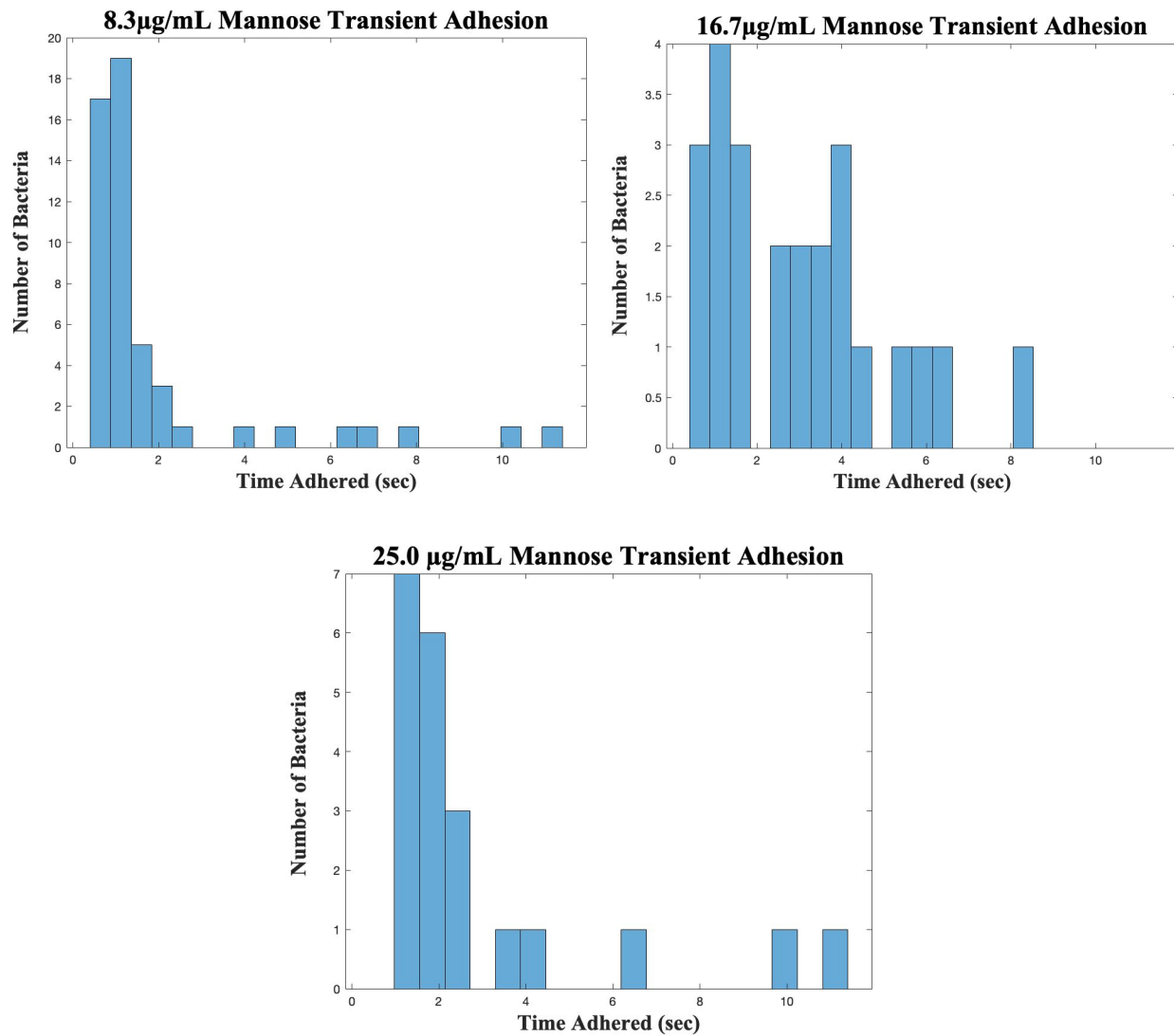
Figure 15 *Distribution of Transient Interaction Times Under Varying Concentrations of Surface*

Immobilized Mannose: Time histograms of transiently interacting bacteria for 8.3µg/mL,

16.7µg/mL, and 25.0µg/mL of BSA-mannose treatment.
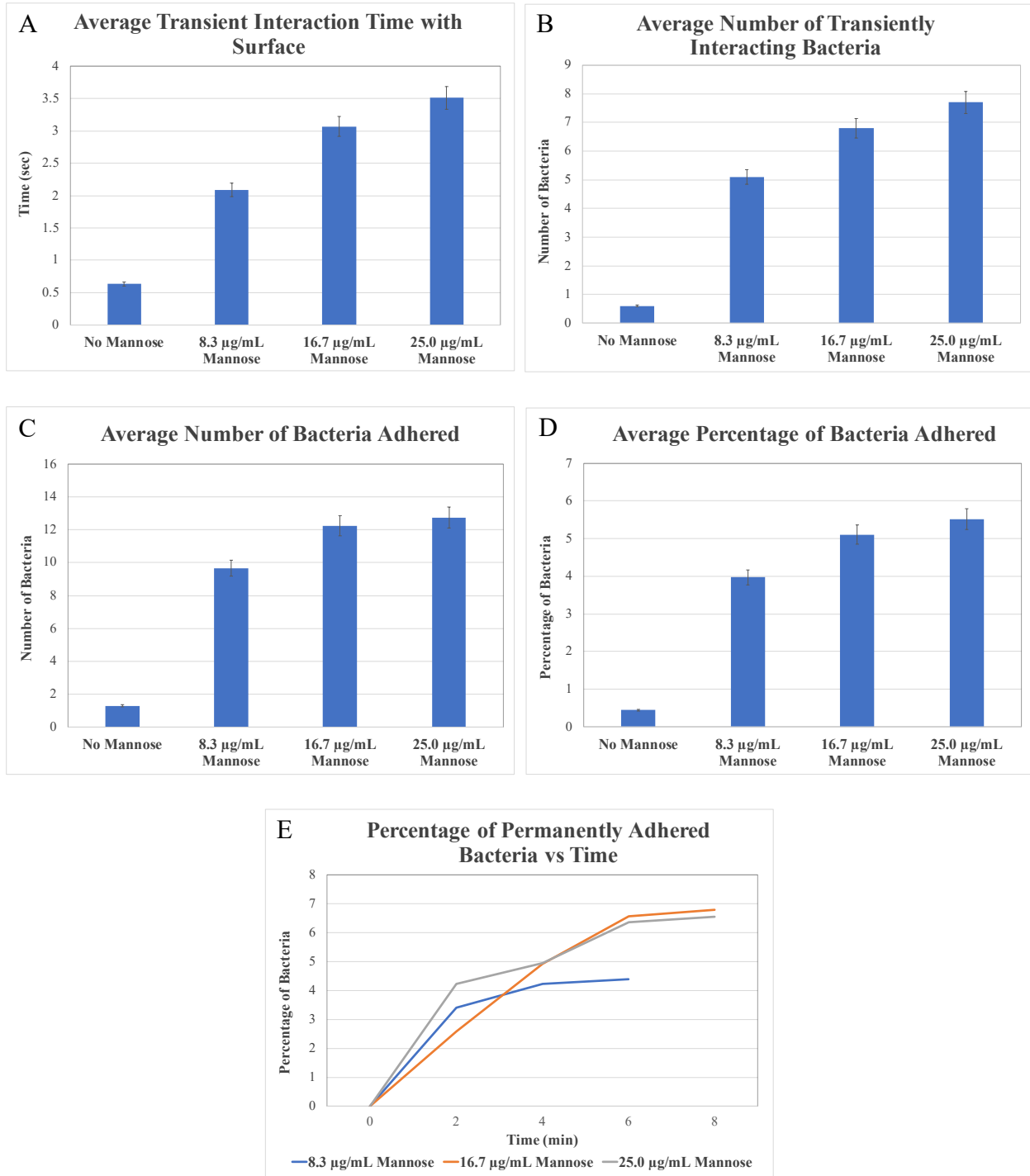
Figure 16 *Analysis of Bacterial Interaction with the BSA-modified Microchannel Surfaces:* A

positive correlation was observed between: (A) BSA-mannose concentration and the average

transient interaction time of bacteria with the device surface, (B) BSA-mannose concentration

and the average number of bacteria transiently interacting with the microchannel surface, (C)

BSA-mannose concentration and the number of bacteria adhered to the microchannel surface, and (D) BSA-mannose concentration and the percentage of bacteria adhered to the device surface. (E) As time increased, the percentage of bacteria permanently adhered to the surface also increased.

3.4 Bacterial Adhesion Results

Bacterial adhesion was observed using microchannels with no BSA-mannose, or functionalized with 8.3µg/mL, 16.7µg/mL, or 25.0µg/mL BSA-mannose solutions. Results indicated that as BSA-mannose concentration increased, the average transient interaction time and the average number of bacteria adhered to the surface also increased (Figure 16). It was also observed that the percentage of permanently adhered bacteria increased overtime across three experimental conditions. Regarding the transient interaction times, the results of a one-way ANOVA indicated a significant difference between the control and mannose-modified microchannels with a significance score of 0.05 ($F_{(3,112)} = 3.745$, $p = 2.7$). This suggests that the interaction between the bacteria and the modified surface was mannose-specific.

CHAPTER 4

DISCUSSION AND FUTURE WORK

4.1 Discussion

In this study, we demonstrated a microfluidic platform mimicking bacterial adhesion to epithelial surfaces to potentially allow for a better understanding of pathogenesis at the mucosal level. Specifically, we cultured an engineered *E. coli* strain that consistently expresses the Type I fimbrial adhesin, FimH. Through agglutination testing, we confirmed mannose-specific clustering of yeast cells by the engineered bacterial strain. A FimH antagonist, mannoside, effectively inhibited agglutination, which indicates the expression of fimbrial lectin. A control experiment with the wild-type strain yielded minimal agglutination, further suggesting that the bacteria were interacting with the yeast through mannose-specific binding. We conclude that the FimHOn strain is expressing the FimH adhesin allowing for mannose-specific interactions.

We observed that the *E. coli* transiently interacted with the mannose-modified surface in a stick-and-roll manner. Bacterial interaction times varied; we observed both short and long adhesion events at the microchannel surface. The mean transient interaction time and the number of bacteria adhered to the surface increased with surface-bound BSA-mannose concentration, indicating mannose-lectin specific binding events at the microchannel surface. We conclude that FimHOn *E. coli* specifically and transiently interacts with the mannose-modified surface.

We also observed that the percentage of permanently adhered bacteria increased as time elapsed, indicating that while the majority of interactions were specific, a small portion of the bacterial population interacted with the surface in a non-specific manner. A small proportion of transient bacterial adhesions can last for longer durations of time, such as tens to hundreds of

seconds. This suggests that longer observation times may be required to accurately distinguish between prolonged specific and non-specific interactions.

4.2 Future Work

While this study demonstrates mannose-specific interaction of type I fimbriated *E. coli*, it would be important to investigate the effect of shear rate on bacterial adhesion by modifying the flow rate of the bacterial solution. Potential correlations can be observed between shear rate and average transient interaction time with the modified surface. Future work can also include testing the effect of inhibitors such as D-mannose and binding pocket mutations on the average transient interaction time with the surface. D-mannose in free solution is thought to prevent *E. coli* from binding to the epithelium, thus preventing bacterial infection (Ala-Jaakkola et al., 2022). The microfluidic platform can be used to observe transient interactions in the presence of various inhibitors. For example, the FimH blocker, TAK-018 inhibits bacterial adhesion to the intestinal epithelium, thereby potentially preventing bowel inflammation (Chevalier et al., 2021). Similarly, a high-affinity FimH inhibitor, M4284, has been shown to reduce bacterial colonization while simultaneously treating urinary tract infections (Spaulding et al., 2017). Testing of such inhibitors could potentially improve our understanding of UTI and IBD pathogenesis and help develop therapeutic approaches.

4.3 Conclusion

Overall, by mimicking molecular interactions and flow-induced shear stress, our microfluidic platform was capable of emulating FimH specific adhesion to mannosylated glycoproteins on mucosal surfaces. Both transient interaction time and the number of bacteria

transiently interacting with the surface increased as a function of surface immobilized mannose concentration. Extensive *in vitro* studies of bacterial-surface interactions within microfluidic platforms can enable future drug discovery and testing of pathogenic *E. coli* strains, and may help explain mechanisms underlying bacterial infections at the mucosal epithelium.

REFERENCES

Ala-Jaakkola, R., Laitila, A., Ouwehand, A.C. *et al.* Role of D-mannose in urinary tract

infections – a narrative review. *Nutr J* 21, 18 (2022). DOI: 10.1186/s12937-022-00769-x

Chevalier, G., Laveissière, A., Desachy, G. *et al.* Blockage of bacterial FimH prevents mucosal

inflammation associated with Crohn's disease. *Microbiome* 9**,** 176 (2021). DOI:

10.1186/s40168-021-01135-5

Chu, C. M., & Lowder, J. L. (2018). Diagnosis and treatment of urinary tract infections across

age groups. *American journal of obstetrics and gynecology*, *219*(1), 40–51. DOI:

10.1016/j.ajog.2017.12.231

Costa, R. F. A., Ferrari, M. L. A., Bringer, M.-A., Darfeuille-Michaud, A., Martins, F. S., &

Barnich, N. (2020). Characterization of mucosa-associated Escherichia coli strains

isolated from Crohn's disease patients in Brazil. *BMC Microbiology*, *20*(1), 1–11. DOI:

10.1186/s12866-020-01856-x

de Souza, H. S., & Fiocchi, C. (2016). Immunopathogenesis of IBD: current state of the art.

Nature reviews. Gastroenterology & hepatology, *13*(1), 13–27. DOI:

10.1038/nrgastro.2015.186

Dreux, N., Denizot, J., Martinez-Medina, M., Mellmann, A., Billig, M., Kisiela, D.,

Chattopadhyay, S., Sokurenko, E., Neut, C., Gower-Rousseau, C., Colombel, J. F.,

Bonnet, R., Darfeuille-Michaud, A., & Barnich, N. (2013). Point mutations in FimH

adhesin of Crohn's disease-associated adherent-invasive Escherichia coli enhance

intestinal inflammatory response. *PLoS pathogens*, *9*(1), e1003141. DOI:

10.1371/journal.ppat.1003141

Edén, C. S., Hagberg, L., Hanson, L. A., Korhonen, T., Leffler, H., & Olling, S. (1981). Adhesion of Escherichia coli in urinary tract infection. *Ciba Foundation symposium*, *80*, 161–187. DOI: 10.1002/9780470720639.ch11

Eshdat, Y., Speth, V., & Jann, K. (1981). Participation of pili and cell wall adhesion in the yeast agglutination activity of Escherichia coli. *Infection and immunity*, *34*(3), 980–986. DOI: 10.1128/iai.34.3.980-986.1981

Fakhoury, M., Negrulj, R., Mooranian, A., & Al-Salami, H. (2014). Inflammatory bowel disease: clinical aspects and treatments. *Journal of inflammation research*, *7*, 113–120. DOI: 10.2147/JIR.S65979

Firon, N., Ofek, I., & Sharon, N. (1984). Carbohydrate-binding sites of the mannose-specific fimbrial lectins of enterobacteria. *Infection and immunity*, *43*(3), 1088–1090. DOI: 10.1128/iai.43.3.1088-1090.1984

Flores-Mireles, A. L., Walker, J. N., Caparon, M., & Hultgren, S. J. (2015). Urinary tract infections: epidemiology, mechanisms of infection and treatment options. *Nature reviews. Microbiology*, *13*(5), 269–284. DOI: 10.1038/nrmicro3432

Foxman, B. (2002). Epidemiology of urinary tract infections: incidence, morbidity, and economic costs. *American Journal of Medicine*, *113*, 5. DOI: 10.1016/S0002-9343(02)01054-9

Gavara N. (2017). A beginner's guide to atomic force microscopy probing for cell mechanics. *Microscopy research and technique*, *80*(1), 75–84. DOI: 10.1002/jemt.22776

Hojati, Z., Zamanzad, B., Hashemzadeh, M., Molaie, R., & Gholipour, A. (2015). The FimH Gene in Uropathogenic Escherichia coli Strains Isolated From Patients With Urinary

Tract Infection. *Jundishapur journal of microbiology*, *8*(2), e17520. DOI: 10.5812/jjm.17520

Kamada, N., Chen, G. Y., Inohara, N., & Núñez, G. (2013). Control of pathogens and pathobionts by the gut microbiota. *Nature Immunology*, *14*(7), 685–690. DOI: 10.1038/ni.2608

Kline, K. A., Fälker, S., Dahlberg, S., Normark, S., & Henriques-Normark, B. (2009). Bacterial adhesins in host-microbe interactions. *Cell host & microbe*, *5*(6), 580–592. DOI: 10.1016/j.chom.2009.05.011

Letourneau, J., Levesque, C., Berthiaume, F., Jacques, M., & Mourez, M. (2011). *In vitro* assay of bacterial adhesion onto mammalian epithelial cells. *Journal of visualized experiments: JoVE*, (51), 2783. DOI: 10.3791/2783

Lu, H., Koo, L. Y., Wang, W. M., Lauffenburger, D. A., Griffith, L. G., & Jensen, K. F. (2004). Microfluidic shear devices for quantitative analysis of cell adhesion. *Analytical chemistry*, *76*(18), 5257–5264. DOI: 10.1021/ac049837t

Martino, P. (2018). Bacterial adherence: much more than a bond. *AIMS microbiology*, *4*(3), 563–566. DOI: 10.3934/microbiol.2018.3.563

Mirelman, D., Altmann, G., & Eshdat, Y. (1980). Screening of bacterial isolates for mannose-specific lectin activity by agglutination of yeasts. *Journal of clinical microbiology*, *11*(4), 328–331. DOI: 10.1128/jcm.11.4.328-331.1980

Mol, O., Oudega, B. (1996). Molecular and structural aspects of fimbriae biosynthesis and assembly in *Escherichia coli*, *FEMS Microbiology Reviews*, Volume 19, Issue 1, Pages 25–52, DOI: 10.1111/j.1574-6976.1996.tb00252.x

Palmela, C., Chevarin, C., Xu, Z., Torres, J., Sevrin, G., Hirten, R., Barnich, N., Ng, S. C., &
Colombel, J. F. (2018). Adherent-invasive *Escherichia coli* in inflammatory bowel
disease. *Gut*, *67*(3), 574–587. DOI: 10.1136/gutjnl-2017-314903

Pizarro-Cerdá, J., & Cossart, P. (2006). Bacterial adhesion and entry into host cells. *Cell*, *124*(4),
715–727. DOI: 10.1016/j.cell.2006.02.012

Razatos, A., Ong, Y.-L., Sharma, M. M., & Georgiou, G. (1998). Molecular Determinants of
Bacterial Adhesion Monitored by Atomic Force Microscopy. *Proceedings of the National
Academy of Sciences of the United States of America*, *95*(19), 11059–11064. DOI:
10.1073/pnas.95.19.11059

Sauer, M., Jakob, R., Eras, J. *et al.* Catch-bond mechanism of the bacterial adhesin FimH.
Nat Commun 7, 10738 (2016). DOI: 10.1038/ncomms10738

Schmidt, H., & Hensel, M. (2004). Pathogenicity islands in bacterial pathogenesis. *Clinical
microbiology reviews*, *17*(1), 14–56. DOI: 10.1128/CMR.17.1.14-56.2004

Secchi, E., Vitale, A., Miño, G.L. *et al.* The effect of flow on swimming bacteria controls the
initial colonization of curved surfaces. *Nat Commun* 11, 2851 (2020). DOI:
10.1038/s41467-020-16620-y

Sharma, V., Ichikawa, M., & Freeze, H. H. (2014). Mannose metabolism: more than meets the
eye. *Biochemical and biophysical research communications*, *453*(2), 220–228. DOI:
10.1016/j.bbrc.2014.06.021

Spaulding, C. N., Klein, R. D., Ruer, S., Kau, A. L., Schreiber, H. L., Cusumano, Z. T., Dodson,
K. W., Pinkner, J. S., Fremont, D. H., Janetka, J. W., Remaut, H., Gordon, J. I., &
Hultgren, S. J. (2017). Selective depletion of uropathogenic *E. coli* from the gut by a
FimH antagonist. *Nature*, *546*(7659), 528–532. DOI: 10.1038/nature22972

Straub, H., Eberl, L., Zinn, M., Rossi, R. M., Maniura-Weber, K., & Ren, Q. (2020). A microfluidic platform for in situ investigation of biofilm formation and its treatment under controlled conditions. *Journal of nanobiotechnology*, *18*(1), 166. DOI: 10.1186/s12951-020-00724-0

Streets, A. M., & Huang, Y. (2013). Chip in a lab: Microfluidics for next generation life science research. *Biomicrofluidics*, *7*(1), 11302. DOI: 10.1063/1.4789751

Tamboli, C. P., Neut, C., Desreumaux, P., & Colombel, J. F. (2004). Dysbiosis in inflammatory bowel disease. *Gut*, *53*(1), 1–4. DOI: 10.1136/gut.53.1.1

Tchesnokova, V., Aprikian, P., Kisiela, D., Gowey, S., Korotkova, N., Thomas, W., & Sokurenko, E. (2011). Type 1 fimbrial adhesin FimH elicits an immune response that enhances cell adhesion of Escherichia coli. *Infection and immunity*, *79*(10), 3895–3904. DOI: 10.1128/IAI.05169-11

Terlizzi, M. E., Gribaudo, G., & Maffei, M. E. (2017). UroPathogenic *Escherichia coli* (UPEC) Infections: Virulence Factors, Bladder Responses, Antibiotic, and Non-antibiotic Antimicrobial Strategies. *Frontiers in microbiology*, *8*, 1566. DOI: 10.3389/fmicb.2017.01566

Thomas W. (2008). Catch bonds in adhesion. *Annual review of biomedical engineering*, *10*, 39–57. DOI: 10.1146/annurev.bioeng.10.061807.160427

Thomas, W. E., Nilsson, L. M., Forero, M., Sokurenko, E. V., & Vogel, V. (2004). Shear-dependent 'stick-and-roll' adhesion of type 1 fimbriated Escherichia coli. *Molecular microbiology*, *53*(5), 1545–1557. DOI: 10.1111/j.1365-2958.2004.04226.x

Tinevez, J.-Y., Perry, N., Schindelin, J., Hoopes, G. M., Reynolds, G. D., Laplantine, E., …
Eliceiri, K. W. (2017). TrackMate: An open and extensible platform for single-particle
tracking. *Methods*, *115*, 80–90. DOI: 10.1016/j.ymeth.2016.09.016

Tuson, H. H., & Weibel, D. B. (2013). Bacteria-surface interactions. *Soft matter*, *9*(18), 4368–
4380. DOI: 10.1039/C3SM27705D

Yakovenko, O., Sharma, S., Forero, M., Tchesnokova, V., Aprikian, P., Kidd, B., Mach, A.,
Vogel, V., Sokurenko, E., & Thomas, W. E. (2008). FimH forms catch bonds that are
enhanced by mechanical force due to allosteric regulation. *The Journal of biological
chemistry*, *283*(17), 11596–11605. DOI: 10.1074/jbc.M707815200